

EOSLT Consortium Biomass Co-firing

WP 4 - Biomass co-firing in oxy-fuel combustion Part II: Ash deposition modelling of coal and biomass blends under air and oxygen combustion conditions

M. Glazer

C.I. Bertrand

L. Fryda

W. de Jong

ECN-E--10-077 JULY 2010

Acknowledgement/Preface

The research work reported in this report was carried out in the frame of EOSLT Consortium Biomass Co-firing with partial financial support from the two RFCS projects: RFCR – CT – 2006 – 00010 (BOFCOM) and RFCR-CT-2007-00009 (ECOSCRUB).

Abstract

An ash deposition modelling study based on the experimental results presented in Part I of this report is presented using the Ash Deposition Predictor (ADP) developed and implemented jointly by TUDelft and ECN. The numerical simulations were performed to answer open questions related to the deposition phenomena for coal and biomass blends and to illustrate any differences between atmospheric combustion conditions and the oxy-fuel combustion. The input data for the model were the series of deposition tests performed under atmospheric and oxyfuel conditions carried out at ECN, described in Part I. During the code validation step, the ADP tool predicted higher deposition ratios for higher viscosity values, in line with literature findings. In addition, the higher calculated fouling index for the lignite coal and blends and as a result the higher fouling propensity are in agreement with the simulation results and the experimental findings for these fuels. A sensitivity analysis on selected code parameters revealed the influence of the PSD on the results generated by the code and in specific on the deposition ratios. The calculations are sensitive to the particle size (PSD) of the collected ashes. In was finally concluded that increased deposition ratios were predicted by the ADP under oxyfuel conditions in comparison to the standard air combustion conditions, while all the other parameters (PSD, viscosity) were kept constant. This result is in agreement with the observed experimental results. However further research is still needed in this respect in (1) further developing the code and (2) the validation of the code.

Contents

List of	tables		4		
List of	figures	3	4		
Nome	nclature	e	5		
Summ	nary		6		
1.	Introdu 1.1 1.2 1.3	uction Scope of the work The Ash Deposition Predictor (ADP) Lab Scale Combustor Simulator (LCS)	8 8 8 9		
2.	Numer 2.1 2.2	rical simulations and settings Modelling with CFD - key settings – CINAR 2.1.1 Calculation domain 2.1.2 Input parameters for CINAR 2.1.3 Oxy-fuel and Air flows per ports 2.1.4 Temperature profile ADP 2.2.1 Simulation programme 2.2.2 Particle trajectory and the deposition process	11 12 12 12 13 13 14 14 14		
3.	Result	2.2.3 Fuels ts and discussion	16 18		
4.		Sensitivity analysis on the influence of the Particle Size Distribution Sensitivity analysis on the influence of the OXY/AIR conditions for a selected fuel	22 22 23		
5.	Conclu	usions and recommendations	25		
Refere	ences		26		
Appen	ndix A	Other CINAR settings OXY-FUEL	28		
Appen	ndix B	Temperature profiles CINAR	29		
Appen	Appendix C ADP – parameters				
Appen	ndix D	Other settings ADP	31		
Appen	ndix E	Ash properties	32		

List of tables

Table 2.1	Simulation CFD CINAR – input for ADP, two environment conditions have been simulated as input for ADP	10
Table 2.2	Gaseous feed composition - oxyfuel (methane, oxygen and carbon dioxide flows).	
Table 2.3	Gaseous feed composition - air (methane, oxygen and nitrogen flows)	
Table 2.4	Simulation cases for the Ash Deposition Predictor	
Table 2.5	Proximate and ultimate analysis of Russian coal, cocoa, lignite and olive residues	
Table 3.1	Deposition ratios for certain viscous elastic properties NBO/T of the deposited ash and the PSD	18
Table 3.2	Particle Size Distribution and the basic to acidic oxides ratio together with the	20
Table 3.3	Fouling index and the deposit ratio for the Russian coal/Lignite and their blends	
Table 4.1	Original and modified deposit ratios for the Russian coal and its blends	
Table 4.2	Deposition ratios for lignite tested under OXY/AIR conditions for cases 1 (upper	
	two rows) and 2 (lower two rows)	23
List of fig	gures	
Figure 1.1	General structure of the Ash Deposition Predictor	<u>c</u>
Figure 1.2	Laboratory Combustion Simulator at ECN	
Figure 2.1	Cases modelled	
Figure 2.2	Numerical mesh – CINAR – deposition probe opening	12
Figure 2.3	The LCS axial temperature profile as function of the distance from the burner	13
Figure 2.4	Ash Deposition Predictor – particle flow visualized by Tecplot, upper left corner –	
	the computational domain with the particles injected, upper right – the numerical	
	mesh in vicinity of the probe, lower left - a particle approaching the probe, lower	40
Figure 2.4	right – the deposit build-up and its thickness	
Figure 3.1	Deposition ratios as a function of NBO/T for the Russian coal and its blends	
Figure 3.2	Deposition ratios as a function of NBO/T for the Lignite and its blends	18

Nomenclature

```
velocity x-axis (m/s)
u
                 velocity y-axis
velocity z-axis
٧
w
                 pressure (Pa / m<sup>-1</sup>·kg·s<sup>-2</sup>)
Ρ
                 temperature (K)
density of a gas (kg/m<sup>3</sup>)
Т
ρ
                 viscosity of gas (1P = 1 g·cm<sup>-1</sup>·s<sup>-1</sup>)
DR
                 Deposition Ratio (-)
                 parameter describing viscous elastic properties of
NBO/T
                 particles (-)
Particle Size Distribution
PSD
                 Ratio of Basic to Acidic oxides
R_{B/A}
\mathsf{F}_\mathsf{f}
                 Fouling factor (Km<sup>2</sup>)/W
```

Summary

The Carbon Capture and Sequestration technologies combining coal/biomass co-combustion under oxyfuel conditions are gaining attention in the last years. This is due to the high CO_2 concentration flue gas streams achieved in this way and the sustainable aspect of biomass use. The produced CO_2 can be sequestered and stored. The high O_2/CO_2 concentrations used for oxyfuel combustion raises questions on the combustion quality (flame, flows, char burnout, corrosion, ash formation and deposition) and heat transfer behaviour when applied to industrial installations. The deposit formation under atmospheric combustion conditions has been subject to numerous investigations and studies and experimental data have identified several chemical and physical processes that control the deposition process. These are inertial impaction, turbulent diffusion, thermophoretic attraction, vapour condensation and heterogeneous reaction between ash particles and deposition surfaces. Previous work on combustion of biomass fuels, especially straw, has revealed challenging issues linked to the formation of submicron aerosols particles, deposits, corrosion and emissions linked in most of the cases to the chemical composition but also to the boiler/combustion characteristics itself.

An ash deposition modelling study has been carried out using the Ash Deposition Predictor (ADP) developed and implemented jointly by TUDelft and ECN. The numerical simulations were performed to answer questions related to the deposition phenomena for coal and biomass blends and to illustrate any differences between atmospheric combustion conditions and the oxy-fuel combustion giving insight into the reasons for the observed differences. In order to provide input data for the model, a series of deposition tests performed under atmospheric and oxyfuel conditions were carried out at ECN, described in Part I of this report. The ADP is a numerical tool which post-processes the data originating from the CFD based modelling of the boiler. The post-processor is an independent particle tracking code which includes inertial impaction, thermophoretic attraction and dynamic reaction of particles on surfaces in order to predict the location of the deposited ash, the growth of the deposit, its characteristics and the impact on heat transfer performance for a given combination of fuel and operating conditions.

During the validation stage of the modelling tool, the ADP predicted more ash deposited for the lower NBO/T (higher viscosity) values which is in agreement with the literature. The higher fouling index for the lignite coal and blends and as a result higher fouling propensity is in agreement with the simulation results and the experimental findings for these fuels. The calculations seem to be sensitive to the particle size (PSD) of the collected ashes as the results reveal. A sensitivity analysis of selected code parameters revealed the influence of the PSD on the results generated by the code and in specific, on the deposition ratios. As final conclusions, increased deposition ratios were predicted by the ADP under oxyfuel conditions in comparison to the standard air combustion conditions, while all the other parameters were kept constant. This result is in agreement with the observed experimental results. However, more work is needed in this respect in (1) further developing the code and (2) the validation of the code.

1. Introduction

The Carbon Capture and Sequestration technologies and in specific, coal/biomass cocombustion under oxyfuel conditions is gaining more and more attention in the last years. This is due to the high CO₂ concentration flue gas streams achieved in this way. The produced CO₂ can be sequestered and stored [Jordal et al., 2005]. The high O₂/CO₂ concentrations used for oxyfuel combustion raises questions on the combustion quality (flame, flows, char burnout, corrosion, ash formation and deposition) and heat transfer behaviour, when applied to industrial installations. Especially the coal biomass co-firing under oxy-fuel conditions and subsequent deposit formation is not yet well understood. The deposit formation under atmospheric combustion conditions has been subject to numerous investigations [Joller et al., 2007; Hindiyarti et al., 2007, Zheng et al., 2006, Fryda et al., 2009]. Theoretical studies and experimental data have identified several chemical and physical processes that control the deposition process. These are inertial impaction, turbulent diffusion, thermophoretic attraction, vapour condensation and heterogeneous reaction between ash particles and deposition surfaces [Joller et al., 2007]. Previous investigations on combustion of biomass fuels, especially straw, has revealed problems linked to the formation of submicron aerosols particles, deposits, corrosion and emissions linked in most of the cases to the chemical composition but also to the boiler/combustion characteristics itself.

1.1 Scope of the work

An ash deposition modelling study has been prepared using the Ash Deposition Predictor (ADP) developed and implemented jointly by TUDelft and ECN [Losurdo, 2009]. The numerical simulations were performed to answer open questions related to the deposition phenomena for coal and biomass blends and to illustrate any differences between atmospheric combustion conditions and the oxy-fuel combustion. In order to provide input data for the model, a series of deposition tests performed under atmospheric and oxyfuel conditions were carried out at ECN, described in Part I and also published [Fryda *et al.*, 2009]. The next paragraphs provide a short description of the ADP together with the experimental equipment (LCS) as present in ECN.

1.2 The Ash Deposition Predictor (ADP)

The ADP is a numerical tool which post-processes the data originating from the CFD based modelling of the boiler. The post-processor is an independent particle tracking code which includes inertial impaction, thermophoretic attraction and dynamic reaction of particles on surfaces in order to predict the location of the deposited ash, the growth of the deposit, its characteristics and the impact on heat transfer performance for a given combination of fuel and operating conditions.

The structure of the Ash Deposition Predictor (ADP) is depicted in Figure 1.1.

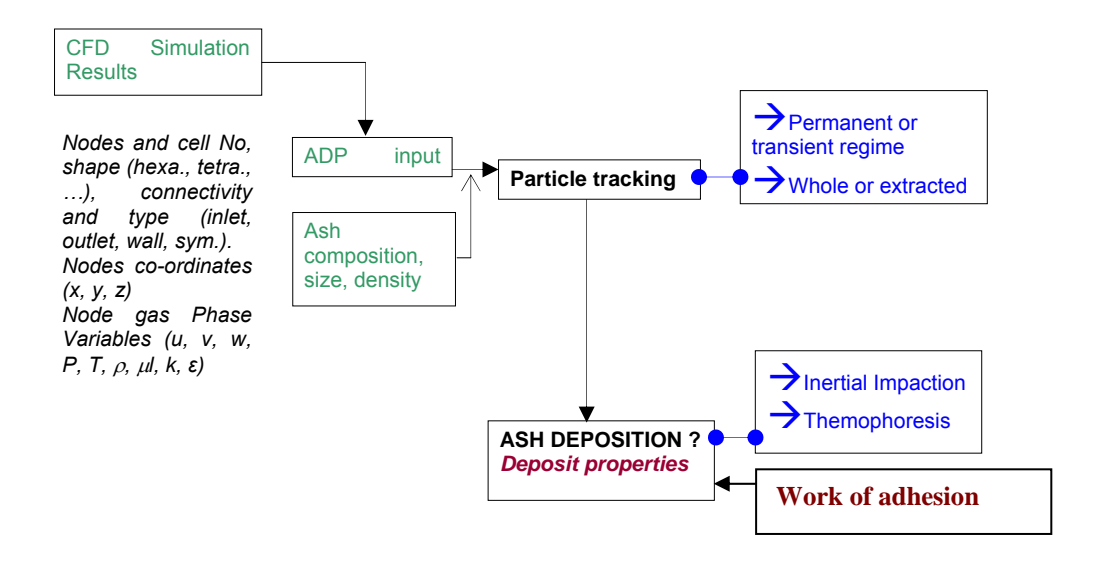


Figure 1.1 General structure of the Ash Deposition Predictor

The ADP encompasses the following steps [Bertrand et al., 2007; Losurdo et al., 2005]:

- The ADP reads and reconstructs hybrid unstructured CFD meshes based on topological node information and associates the values of the gas phase variables (for example: u, v, w, P, T, ρ) together with the position of the inlet(s), outlet(s), wall and potential symmetries in the domain.
- The modeller can select the particles injection point(s) or, simply, particles are randomly injected through the inlet ports and tracked in a steady or unsteady manner according to a Lagrangian Frame through the complete and/or a reduced computational domain.
- A Real Time Deposit Evaluation (RTDE) algorithm allows deposit properties like thickness, temperature, viscosity, composition and thermal resistance to be evaluated during the course of the tracking process and updated in real time to predict the changes that may occur on the deposit surface when tracking is in progress in a transient regime.

1.3 Lab Scale Combustor Simulator (LCS)

The numerical calculations using the ADP were performed in order to evaluate the experimental data obtained from a series of ash deposition experiments in the Lab-scale Combustion Simulator (LCS) shown in Figure 1.2, using a special deposition probe, and to further develop and validate the code itself with new experimental data.

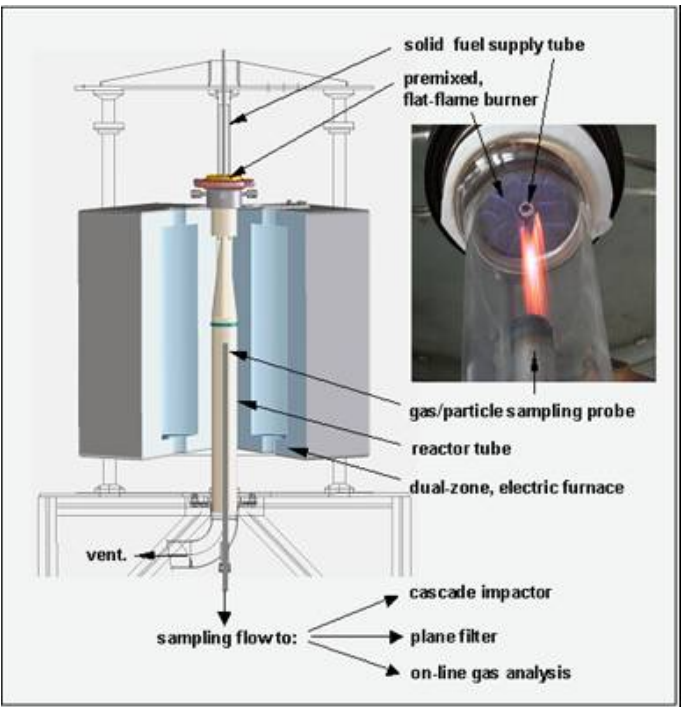


Figure 1.2 Laboratory Combustion Simulator at ECN

The ECN LCS consists of a drop tube reactor with an integrated, premixed and multistage flat flame gas burner. The staged gas burner accommodates high initial heating rates and temperatures and provides the possibility to simulate air staging as in low-NO_x burners and also the presence of specific combustion products such as, e.g., SO₂. Fuel particles (or in specific cases, glass particles) are fed through the inner burner and are rapidly heated (>10⁵ °C/s) to the high temperature level of, e.g., a coal flame (1400-1600°C). The particles travel down with the gas through an alumina reactor tube whilst combusting. The reactor tube is externally heated by a two/three staged ceramic furnace.

An oil cooled probe is used for sampling char and ash at several locations along the reactor vertical axis and a thermally controlled probe simulating a boiler super heater tube is inserted horizontally at the base of the system. The LCS setup is described in detail elsewhere [Korbee et al., 2003].

2. Numerical simulations and settings

The scope of the work was the ash deposition simulation of two fuels (Russian coal and Greek lignite and their blends with cocoa and olive residues respectively (Figure 2.1).

A CFD modelling tool called CINAR® has been used in order to perform the CFD calculations. CINAR is a commercial code developed by the group of F. Lockwood at Imperial College (London) and has been used to numerically model industrial combustion boilers [Lockwood *et al.*, 2002]. A numerical mesh was built using the mesh generator which is part of the CINAR code. The mesh reconstructs the geometry of the LCS. Special attention has been paid to the deposition probe where the mesh has been defined in more detail (see Figure 2.1).

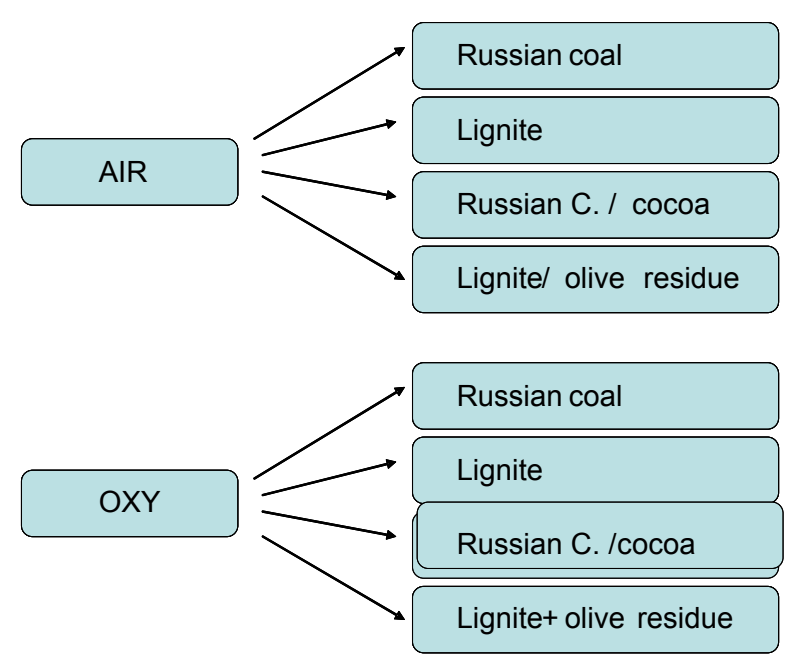


Figure 2.1 Cases modelled (based on the experimental work – Part I).

The CFD calculations have been performed for two different operational conditions, namely air combustion and oxy-fuel combustion environment. For each of these settings the flows and concentrations of the process (flue) gases, the reactor temperature profiles and the physical properties of the gas have been specified so as to reflect the conditions used during the LCS experiments. As a result of the CFD simulations a flow field has been calculated. For this flow field a set of characteristic parameters has been obtained, namely velocities, pressure, temperature distribution, etc. within the numerical domain. This flow field has been used as input for the ADP to perform the deposition calculations.

2.1 Modelling with CFD - key settings - CINAR

2.1.1 Calculation domain

The numerical mesh has been built in three dimensions and consists of 52332 nodes and 46720 cell elements representing the real scale LCS. The numerical mesh applied allows applying accurately numerical calculations with a reasonable trade off between the calculation accuracy (numerical convergence) and the time of calculation. In the vicinity of the probe an opening in the numerical mesh has been refined (see Figure 2.2).

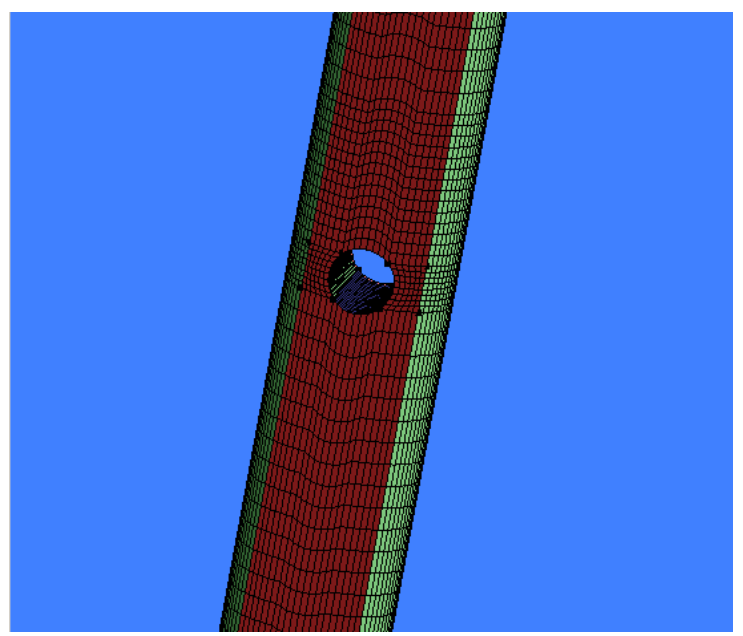


Figure 2.2 Numerical mesh – CINAR – deposition probe opening

2.1.2 Input parameters for CINAR

The CFD calculations with the CINAR code have been performed for two different combustion regimes. Namely, the oxy-fuel combustion regime and the standard (or reference) atmospheric combustion conditions (see Tables 2.1-2.3) have been applied. These conditions were used during the experiments at LCS, comparing modelling and experimental results. This will help, first, to interpret and evaluate the observed experimental findings, based on the physical phenomena included in the model and second, after having acquired a solid background on the phenomena simulated in the ADP and possibly improve further the code, the validation of the ADP tool can take place. In its final form, the model will be a tool for predicting the ash deposition phenomena in large scale combustors for designing or facility modification purposes.

Table 2.1 Simulation CFD CINAR – input for ADP, two environment conditions have been simulated as input for ADP

CFD – code	ENVIRONMENT
CINAR	AIR
CINAR	OXY

2.1.3 Oxy-fuel and Air flows per ports

The combustion gases (CH₄, O₂ and CO₂) for the inner and the outer burner as well as the ring for the oxyfuel case were specified as follows, in order to achieve standard combustion conditions – 3-4% of O₂ in the flue gas exit (Table 2.2 and 2.3):

Table 2.2 Gaseous feed composition - oxyfuel (methane, oxygen and carbon dioxide flows)

	Port	Port	Port	Total Flow	Total Flow	Total Flow
OXY-FUEL	inner(I/min)	outer(I/min)	ring(l/min)	l/min	g/min	moles/min
CH₄	0.300	3.220	0.000	3.520	2.513	0.157
O_2	0.550	8.000	0.000	8.550	12.207	0.381
CO ₂	1.200	18.000	1.670	20.870	40.969	0.931
			SUM	32.940	55.688	

The methane, oxygen and nitrogen streams for the inner, outer burner and the ring in the air case have been specified as follows:

Table 2.3 Gaseous feed composition - air (methane, oxygen and nitrogen flows)

	Port	Port	Port	Total Flow	Total Flow	Total Flow
AIR	inner(I/min)	outer(I/min)	ring(l/min)	l/min	g/min	moles/min
CH ₄	0.180	2.350	0.000	2.530	1.806	0.113
O ₂	0.300	5.600	0.000	5.900	8.423	0.263
N_2	1.100	21.000	1.670	23.770	29.694	1.060
			SUM	32.200	39.923	

The above presented flows reflect the conditions used during the experiments.

2.1.4 Temperature profile

The reactor wall temperature profile was determined iteratively so that the modelled axial temperature profile matches the temperature profile measured with a thermocouple on the axis of the LCS combustor during the experiments for the oxy-fuel and air combustion conditions (Figure 2.3).

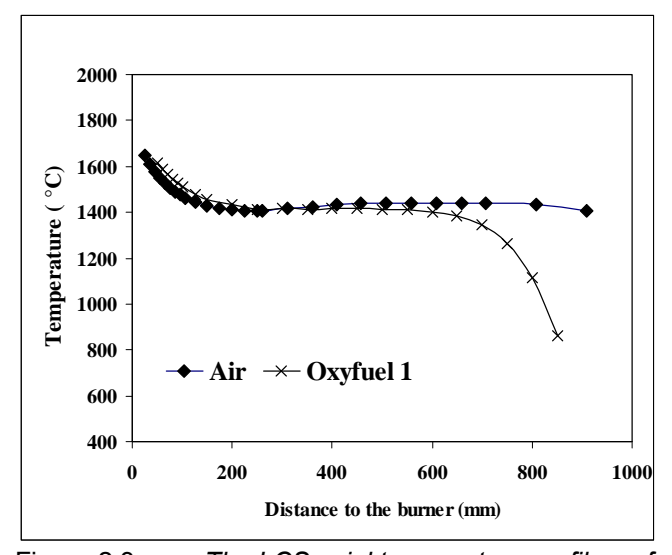


Figure 2.3 The LCS axial temperature profile as function of the distance from the burner

The methodology to determine the wall temperature as input for the CFD was as follows: a set of wall temperatures was assumed as a boundary condition and iterations were performed in the CINAR code until it resulted in the same modelled and measured axial temperatures. Those profiles were continuously compared and if necessary, corrections were applied until for a given set of wall temperatures a matching with the experimentally obtained axial profile was obtained.

2.2 ADP

2.2.1 Simulation programme

The simulation case matrix follows the LCS experimental data available for the selected coals, biomass and blends. The fuels used were

- Russian coal
- Lignite

and their blends with biomass

- Russian coal / cocoa
- Lignite /olive residues

The simulations were performed for the "reference" air combustion conditions and for the oxy-fuel conditions, aiming to observe the differences in deposition phenomena for these two combustion conditions. The simulation cases are summarized in Table 2.4.

Table 2.4 Simulation cases for the Ash Deposition Predictor

Experiment number/ADP number	Environment	Fuel
LCS373	AIR	Russian coal
LCS316	OXY	Russian coal
LCS374	AIR	Russian coal/cocoa
LCS317	OXY	Russian coal/cocoa
LCS441	AIR	Lignite
LCS449	OXY	Lignite
LCS446	AIR	Lignite/olive residue
LCS448	OXY	Lignite/olive residue

2.2.2 Particle trajectory and the deposition process

The particles are introduced in the ADP model. In total, the flow and the deposition of 10000 particles have been simulated. The calculation process is a trade-off between the deposition accuracy (more particles involved) and the computation time. At this moment for 10000 particles injected the calculation time for one test equals approx. 2 weeks. For the ADP certain physical properties of the particles were specified (for more details see Appendix 3).

Key parameters are:

- particle size distribution (PSD) with the mean diameter
- particle density
- particle composition based on SiO₂ molar fraction
- particle viscous elastic properties NBO/T (ratio of non-bridging oxides to tetrahedral oxygen)
- Young module

The viscous elastic properties of the ash particles have been specified based on the NBO/T formula proposed by [Senior *et al.*, 1994]. The NBO/T is the ratio between the non bridging oxygen and the tetrahedral oxygen [Senior *et al.*, 1995] and is given by the general formula (equation 1):

$$NBO/T = \frac{FeO + CaO + MgO + K_2O + Na_2O - Al_2O_3 - FeO_3}{(SiO_2 + TiO_2)/2 + Al_2O_3 + Fe_2O_3}$$

Equation 1 - NBO/T formula

The NBO/T is a parameter developed to predict the viscosity of individual coal ash particles at the temperatures and velocities typically found in coal-fired utility boilers and in comparison to the other models accurately predicts the viscous elastic properties within the higher viscosity ranges. In addition, the model for NBO/T predicts better the viscosity for certain compositions which are commonly found in ash particles [Senior *et al.*, 1995; Srinivasachar *et al.*, 1992].

Some of the parameters have been assumed to be constant for all the calculations (for example Young module) while some others were assumed particle specific (PSD, NBO/T) and defined specifically for each of the modelling runs. The importance and the influence of NBO/T are discussed in relation to other results further on.

In order to characterize the deposition propensity of the fly ash the ash composition as collected on the filter and on the deposition probe was taken into account. The composition of the filter ash and the ash deposited on the deposition probe were thought to better represent the state of the particles at the moment of deposition and is origination directly from the corresponding experiments. The exact composition of the filter/deposition probe ashes can be found in Appendix 5. Particle density was kept constant for all tests and assumed to be 1900 kg/m³.

The visualization of the particle injection process together with the particle flow and the deposition on the probe is presented in Figure 2.4.

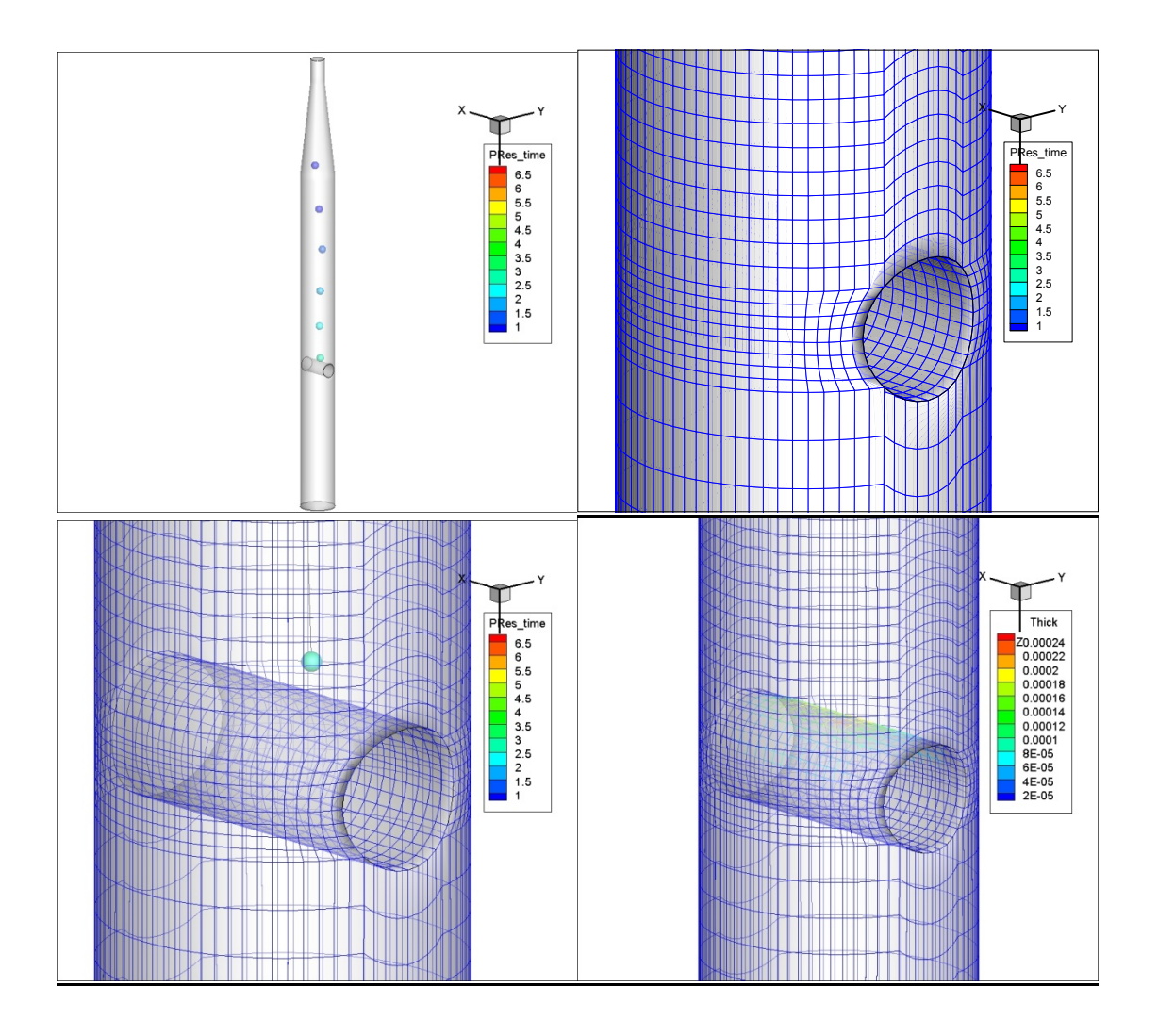


Figure 2.4 Ash Deposition Predictor – particle flow visualized by Tecplot, upper left corner – the computational domain with the particles injected, upper right – the numerical mesh in vicinity of the probe, lower left - a particle approaching the probe, lower right – the deposit build-up and its thickness

2.2.3 Fuels

The numerical study of ash deposition was carried out for two coals (Russian and Lignite) and their blends with cocoa and olive residues (ground). The proximate and ultimate analyses together with the analysis of the inorganic matter are presented in Table 2.5.

Lignite is characterised by high ash content at the level of 42%. The ash content for the Russian coal is much lower at 14.9%. The concentration of the fouling elements like potassium in lignite is 4 times higher than in the Russian coal. Silica content is also much higher for the lignite than for the Russian coal. Based on these concentrations much more deposit formation relative to the thermal conversion of lignite can be expected. This fact was observed during the experiments with lignite. Also the cocoa is characterized by very high potassium content but opposite to the Russian coal the silica content is much lower. The potassium content in the olive residue is also relatively high.

Table 2.5 Proximate and ultimate analysis of Russian coal, cocoa, lignite and olive residues

Fuel	Russian coal	Cocoa	Lignite	Olive residue
Moisture	3.4	11.1	35.8	5.8
ash @ 815°C	analysis (% mass 15	, dry fuel ba	asis) 43	6
Volatile matter	29	62	38	72
			13700	20000
HHV (KJ/kg)	27800	19410	13700	20000
Initial Deformation (°C)	1250	1140		
Hemisph. Temperature (°C)	1360	1310		
Flow Temperature (°C)	1410	1330		
Ultimate a	nalysis (% mass,	drv fuel ba	sis)	
С	68	49.4	33	48
Н	4.0	5.3	2.7	5.7
N	0.9	2.6	0.6	1.1
S	0.3	0.3	0.8	0.1
O by diff.	11.6	40.1	18.8	38
Ash com	oosition (mg/kg fo	ual dry has	ie)	
Na (± 7)*	405	179	1600	1300
Mg (± 1)	1277	1937	5500	1800
AI (± 4)	16583	772	34000	1200
Si (± 90)	34841	1861	64000	6200
P (± 15)	386	1684	110	620
K (± 20)	2390	20790	6600	8900
Ca (± 20)	2750	2140	7100	13000
Ti (± 8)	622	47	1400	76
Mn (± 6)	89	24	200	35
Fe (± 4)	6077	1095	15000	1800
Zn (± 1)	21	4	50	12
Pb (± 20)	10	0	25	25
Sr (± 5)	183	18	59	15
Ba (± 5)	260	22	150	11
CI (± 20)	100	800	47	2000

Results and discussion.

The deposition ratios have been defined as the ratio between the ash deposited to the ash fed in the reactor via the fuel:

DR = (kg ash deposited)/(kg ash fed)

The deposition ratio (= capture efficiency) together with the number of particles which actually have deposited for the calculated sets of NBO/T parameters are presented in Table 3.1 and Figures 3.1 and 3.2.

In general the deposition ratios are lower for the Russian coal and its blends than for the Lignite blends. The reason for it maybe the lower content of silica, potassium and calcium. One has to remember that the numerical modelling predicts the behaviour in this case of coal ashes under certain assumptions and according to the defined parameters. In case of the Ash Deposition Predictor the viscous elastic properties are evaluated based on the NBO/T parameter.

Table 3.1 Deposition ratios for certain viscous elastic properties NBO/T of the deposited ash and the PSD

	don and the rot				
Test	Environment	Fuel	NBO/T	Deposition ratio	PSD (m)
LCS373	AIR	Russian coal	-0.1810	0.3462	4.651E-05
LCS316	OXY	Russian coal	-0.18067	0.2774	2.776E-05
LCS374	AIR	Russian coal/cocoa	-0.27077	0.3384	4.380E-05
LCS317	OXY	Russian coal/cocoa	-0.28346	0.311	3.300E-05
LCS441	AIR	Lignite	-0.08448	0.3081	3.860E-05
LCS449	OXY	Lignite	-0.1004	0.5965	8.600E-05
LCS446	AIR	Lignite/olive residue	-0.0058	0.2972	3.994E-05
LCS448	OXY	Lignite/olive residues	-0.02133	0.3506	4.863E-05

The NBO/T parameter can take either positive or negative values. A strongly negative value indicates lower viscosities (ash less sticky). As reported in the literature, in silicate melts of geologic interest and bulk coal ash compositions the NBO/T is positive. However, in many individual coal ash particles, particularly in those with high content of aluminosilicate clays, the NBO/T is negative (less sticky). Thus the NBO/T values are coal-specific and the negative values indicate a high alumina content.

The composition of the ashes after the fuel combustion has been taken for each experiment respectively. The NBO/T for the Russian coals is strongly negative. NBO/T can take values which are lower than zero which indicates "glasses" in which there is insufficient amount of modifier ions to stabilize Al³⁺ or Fe³⁺. Aluminium seems to behave as a network modifier modifying ions in such structures. According to [Senior *et al.*, 1995] the viscosity measurements show that increasing the amount of aluminium where NBO/T is less than zero actually decreases the viscosity.

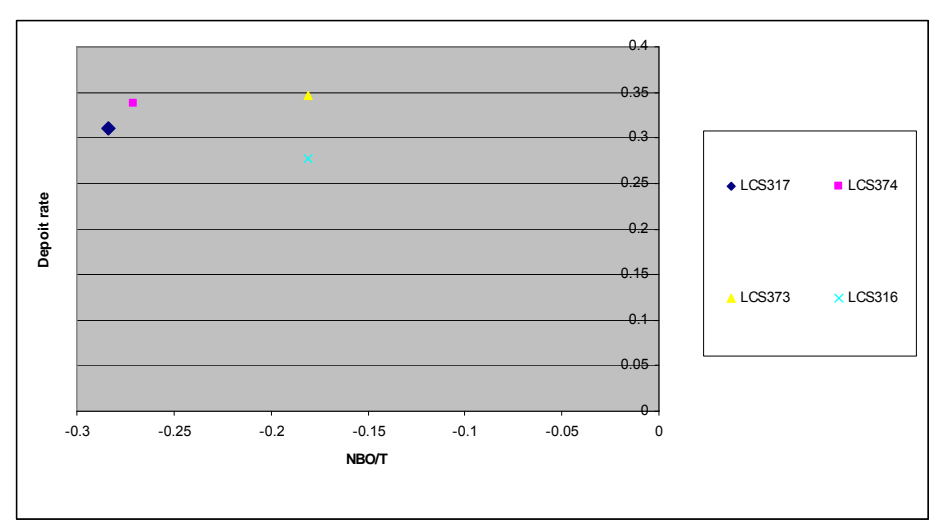


Figure 3.1 Deposition ratios as a function of NBO/T for the Russian coal and its blends

This could suggest that the Russian coal ashes are less sticky according to the model used in the ADP, which justifies the lower deposition ratios as well. The NBO/T values for lignite are closer to zero thus indicating more sticky deposits. In addition to NBO/T the ADP uses the ratio between calcium oxide and aluminium oxide to describe the viscous elastic properties but influence of this parameter is not discussed in this report.

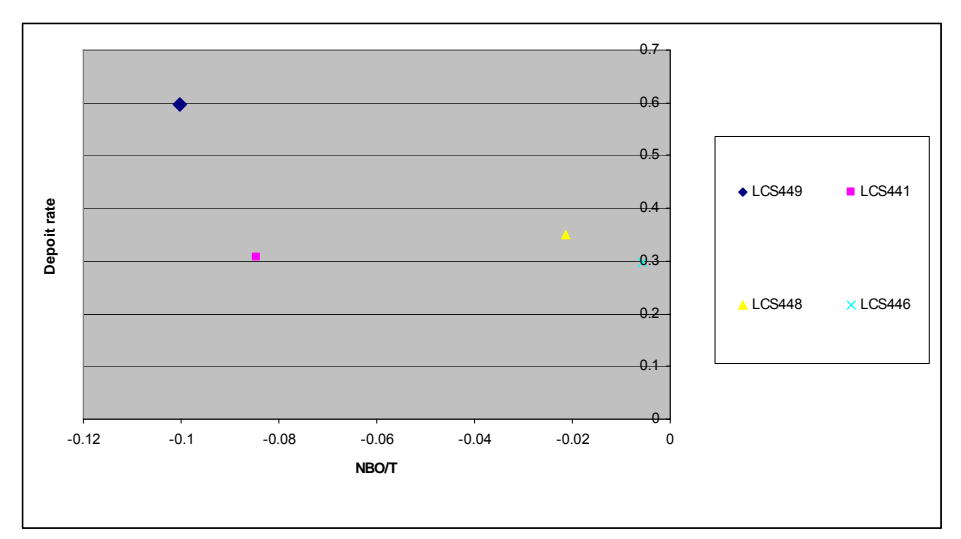


Figure 3.2 Deposition ratios as a function of NBO/T for the Lignite and its blends

According to Doshi *et al.* 2009, the inorganics present within biomass and coal that are of concern during ash formation and further on during the deposit formation can be classified into 3 groups. The first two groups are the ionically and organically bound inorganics, which are mainly found in biomass and the third group is the minerals found both in coal and biomass. Glazer (2007) in his PhD thesis showed clear effects of interactions of inorganics present in biomass with those present in coal during the biomass coal co-firing. The high temperature gas chemistry seems to reduce the release of the alkali metals transforming them into less harmful and sticky alkali-alumina-silicates [Jimenez *et al.*, 2007]. The NBO/T and the ratio of basic to acidic oxides R_{B/A} (equation 2) give an indication about the possible real life behaviour of the tested fuels. Higher

values of $R_{\text{B/A}}$ together with the negative but close to zero NBO/T value, indicates strong fouling propensity.

Ratio of basic to acidic oxides:

$$R_{B/A} = \frac{Fe_{2}O_{3} + CaO + MgO + K_{2}O + Na_{2}O}{SiO_{2} + Al_{2}O_{3} + TiO_{2}}$$

Equation 2 - Ratio of basic to acidic oxides

The $R_{B/A}$ ratios for the Russian coal and its blends are substantially lower indicating the higher share of the alumino-silicates within the system (Table 3.2). A low value also indicates low concentration of K/Na/Mg/Ca elements forming basic oxides.

Table 3.2 Particle Size Distribution and the basic to acidic oxides ratio together with the NBO/T and the deposition ratio for the Russian coal/Lignite and their blends

Test	Environment Fuel		NBO/T	R B/A	PSD (m)	Deposition ratio
LCS373	AIR	Russian coal	-0.18107	0.14415	4.651E-05	0.3462
LCS316	OXY	Russian coal	-0.18067	0.13422	2.776E-05	0.2774
LCS374	LCS374 AIR Russian coal/cocc		-0.27077	0.19173	4.380E-05	0.3384
LCS317	OXY	Russian coal/cocoa	-0.28346	0.18306	3.300E-05	0.311
LCS441	AIR	lignite	-0.08448	0.24622	3.860E-05	0.3081
LCS449	OXY lignite		-0.1004	0.23778	8.600E-05	0.5965
LCS446	LCS446 AIR Lignite/olive residue		-0.0058	0.30386	3.994E-05	0.2972
LCS448 OXY		Lignite/olive residue	-0.02133	0.2871	4.863E-05	0.3506

Another index that describes the fouling behaviour of fuels is the Fouling Index (equation 3). The fouling index is defined as the ratio between potassium and sodium to chlorine and sulphur, as the main fouling responsible elements. The fouling index in this case has been calculated on basis of the composition of the collected ash deposits and not the fuel composition as is the case with the previously described ratios. Interesting findings are revealed when looking closer at the fouling index of the fuels and their blends. It can be seen that for the oxyfuel combustion conditions the fouling index is higher both for the Russian coal and the lignite, in comparison to the air combustion cases. On the other hand the direct relation between the fouling index and the deposition ratios is profound in the case of lignite and its blends. The results including the fouling index, together with all the previous parameters are shown for comparison in Table 3.3. In general for lignite and its blends the fouling index is much higher than for the Russian coal, which is related to the high content of potassium and sodium. Interesting is the observation that for the oxyfuel environment the fouling index is higher than for air combustion. This indicates that the ash composition varies with the combustion environment.

$$F_f = \frac{K + Na}{Cl + 2S}$$

Equation 3 - Fouling index

The fouling index is not the last parameter that may help in describing the deposition phenomena but it is considered an important one [Wei et al., 2002]. The ADP code relies on the input data as provided by the experiments; the fouling factor as defined here does not form an input to ADP currently. According to [Lokare et al., 2006] ash impaction efficiency depends on particle density and size, whereas capture efficiency mainly depends on particle composition thus on elemental composition which in the end determines the viscous elastic properties.

It has to be stressed that the ADP in it current form is a particle tracking tool with the extended full impaction and thermophoretic attraction functionalities based on the specified viscous elastic properties of the particles and does not take into account the chemical interactions neither in the gas phase nor in the gas-liquid-solid phase taking place in real cases [Korbee et al. 2007].

Table 3.3 Fouling index and the deposit rate for the Russian coal/Lignite and their blends

1 4016 3.3	Tourng maex and the deposit rate for the Russian coarcignite and their blends							
Test	Environment	Fuel	NBO/T	R _{B/A}	PSD (m)	Deposition ratio	Fouling index - F _f	
LCS373	AIR	Russian coal	-0.18107	0.14415	4.651E-05	0.3462	0.874	
LCS316	OXY	Russian coal	-0.18067	0.13422	2.776E-05	0.2774	2.031	
LCS374	AIR	RC/cocoa	-0.27077	0.19173	4.380E-05	0.3384	1.637	
LCS317	OXY	RC/cocoa	-0.28346	0.18306	3.300E-05	0.311	2.603	
LCS441	AIR	Lignite	-0.08448	0.24622	3.860E-05	0.3081	14.087	
LCS449	OXY	Lignite	-0.1004	0.23778	8.600E-05	0.5965	21.198	
LCS446	AIR	Lignite/olive residue	-0.0058	0.30386	3.994E-05	0.2972	15.634	
LCS448	OXY	Lignite/olive residue	-0.02133	0.2871	4.863E-05	0.3506	42.7	

The investigated deposition phenomena form a multi parameter system where many factors may influence the observed behaviour. On one hand the NBO/T ratio describing the viscous elastic properties indicates that all the coals and coals blends are rich in alumina but one the other hand does not give definitive explanation for the deposition phenomena. The PSD of the particles indicates a relation between the particle size and the deposition ratio (larger particles more deposits). In addition the analysis of the fouling indexes and the deposition ratios reveals strong relationship in the case of lignite. In order to differentiate between the influencing factors some sensitivity analysis was performed.

4. Sensitivity analysis

4.1 Sensitivity analysis on the influence of the Particle Size Distribution

In order to test the sensitivity of the ADP to the ash particle sizes (PSD) of the collected ash samples, the original numerical calculations have been repeated with modified PSD values. In the modified case, the PSD of the lignite coal and blends has been used as the input parameter for all cases, replacing the PSD values for the Russian coal test cases. It means that for the Russian coal cases, all the other input parameters were the ones for the Russian coal and its blends but the PSD has been replaced by the lignite cases, rendering the PSD is homogeneous for all the runs. From these results it is clearly visible that the PSD has a profound influence on the results (Table 4.1).

Table 4.1 Original and modified deposit ratios for the Russian coal and its blends. The PSD of the lignite coal and blends has been used as the input parameters for ADP

of the lignite coal and blends has been used as the input parameters for ADP								
Test	Environment	Fuel	DR original	DR modified	PSD original	PSD modified	NBO/T	
LCS373	AIR	Russian coal	0.3462	0.3078	4.651E-05	3.860E-05	-0.18107	
LCS316	OXY	Russian coal	0.2774	0.5950	2.776E-05	8.600E-05	-0.18067	
LCS374	AIR	Russian coal/cocoa	0.3384	0.3247	4.380E-05	3.994E-05	-0.27077	
LCS317	OXY	Russian coal/cocoa	0.311	0.3962	3.300E-05	4.863E-05	-0.28346	
LCS441	AIR	lignite	0.3081	0.3081	3.860E-05	3.860E-05	-0.08448	
LCS449	OXY	lignite	0.5965	0.5965	8.600E-05	8.600E-05	-0.1004	
LCS446	AIR	Lignite/olive residues	0.2972	0.2972	3.994E-05	3.994E-05	-0.0058	
LCS448	OXY	Lignite/olive residues	0.3506	0.3506	4.863E-05	4.863E-05	-0.02133	

With the PSD being replaced for the Russian coal the trend is different for both the Russian coal and its blends. In the case of the modified PSD the oxyfuel combustion seems to lead to more deposit production, in a similar trend as the lignite cases. This trend was also observed during the experiments where the oxyfuel tests resulted in larger deposition ratios. In addition, it can be observed that the modified deposition results are almost identical to the ones of lignite indicating again a strong PSD input influence in the deposition phenomena (impaction mechanism encompassed in the code).

According to [Joller et al., 2007] inertial impaction on boiler tubes is relevant mainly for coarse particles, since aerosols will follow the gas flow. For the aerosols thermophoresis phenomena may play a role as well. This explains the strong influence of the PSD on the deposition behaviour. Larger particles are more prone to impact on the boiler tube; therefore, a direct link can be made, between larger particles and larger deposition ratios.

The proper PSD estimation is critical in order to define the relevant deposition formation mechanisms during the combustion of coal and biomass. In addition to particle formation and the deposit formation process, direct condensation of aerosols forming species on furnace walls and in this case on the deposition probe must be considered. The probe during the experiments was kept at 600°C. Unfortunately this phenomena was not modelled within this version of the ADP. In the newer version of the ADP, "equivalent condensation" phenomena could be modelled by considering very small aerosol particles that deposit to the surface by thermophoresis. However these aerosol particles have much different viscous-elastic properties than fly ash. It would mean that another set of viscous-elastic properties would need to be considered in the ADP.

4.2 Sensitivity analysis on the influence of the OXY/AIR conditions for a selected fuel

The lignite is characterised by a very high ash content which renders it suitable for the deposition tests and the numerical study. In order to test the sensitivity of deposition ratio within the code for the given OXY and AIR combustion conditions the following cases were considered:

- 1. PSD identical, but other parameters like NBO/T test specific
- 2. PSD as well as other parameters like NBO/T identical

Especially the second case is expected to provide information how the different flow field for the oxyfuel conditions (temperature, pressure and gas distribution together with different velocity vectors) influence the deposition process for the same fuel chemical composition (reflected in NBO/T) and the same PSD. The results of the cases mentioned are shown in Table 4.2.

Table 4.2 Deposition ratios for lignite tested under OXY/AIR conditions for cases 1 (upper two rows) and 2 (lower two rows)

Test	Environment	Fuel	Deposition ratio original	Deposition ratio modified	PSD (m) original	PSD modified	NBO/T
LCS441	AIR	lignite	0.3081	0.5497	3.860E-05	8.600E-05	-0.0845
LCS449	OXY	lignite	0.5965	0.5965	8.600E-05	8.600E-05	-0.1004
LCS441	AIR	lignite	0.3081	0.5548	3.860E-05	8.600E-05	-0.0924
LCS449	OXY	lignite	0.5965	0.5944	8.600E-05	8.600E-05	-0.0924

The first case, (Table 4.2, first 2 lines), where the PSD are equal but all the other parameters including the NBO/T are test specific, reveals and confirms the relationship between the lower NBO/T and the increased deposition ratios. From the second case it is visible from table 4.2 that the deposition ratios are slightly higher for the oxyfuel conditions where all the other parameters are the same. A possible explanation for this is the altered flow fields, in other words, the gaseous flow lines and the physical properties of the gaseous environment in general, under the given temperature regime, which affects finally the deposition behaviour. This is in agreement with the experimental

findings [Fryda *et al.*, 2009] and is the subject of other published works [PhD, Shrinivas S. Lokare, 2008].

The agreement between the tests and the code results is encouraging for the further development of the ADP code.

The possible explanation for the systematic shift towards larger deposition ratios under oxyfuel conditions observed during the experiments could be due to (a) larger particle formed under oxyfuel, which promotes the inertial impaction of ash on a surface, and (b) the different viscosities of the gaseous environments: the $N_2/O2$ in the air combustion and the CO_2/O_2 during the oxyfuel combustion. The viscosity of air is slightly larger than the viscosity of CO_2 (μ_{CO2} = 0.0001371 Poise against μ_{air} = 0.0001675 Poise), while the densities of the gases follow the opposite trend (CO_2 is heavier, denser than air).

These aerodynamics parameters affect the flow field and the way ash particles behave in that flow field and therefore seem to affect the impaction efficiency of the ash particles, as they influence the flow dynamics of the described phenomena. For the same particle sizes of the ash, the higher viscosity of air is probably the answer to the lower deposition ratios observed, as explained theoretically by Lokare [2009].

The particle size distribution plays a significant role as well, as very small particles will not easily impact the surfaces, because they will be carried away by the gas flow. Therefore, in this case, for the same gas (same viscous behaviour), and for the same gas velocity as well, larger particles are more prone to impact on the surfaces, as they will not follow the flow field around the deposition tube (deposition surface).

Naturally, the chemical composition of particles must not be neglected, as it affects the final capture efficiency, in other words, the final amount of ash that will stick and remain on the probe. This is partly dependent on ash chemistry and partly dependent on the particle geometry and target surface characteristics. In the ADP, the target surface as well as the particle characteristics were not variable parameters, therefore their influence was not studied. The chemical characteristics of the ash have been taken into consideration of course, through the parameters described in the relevant paragraphs: NBO/T, fouling index, $R_{A/B}$.

5. Conclusions and recommendations

A set of numerical calculations has been performed using the Ash Deposition Predictor in order to assess the deposition formation behaviour during the combustion of two types of coal and their blends under oxyfuel and standard air combustion atmospheres.

The ADP tool predicted more ash deposited for the lower viscous elastic values (the ratio between the non bridging oxygen and the tetrahedral oxygen) which is in agreement with the literature. Furthermore, the formation of less sticky deposits indicates the positive influence of the alumina-silicates in the ash.

The fouling index is much higher for the lignite coal and its blends giving an additional explanation to the numerical findings. The higher fouling index for the lignite coal and blends and as a result higher fouling propensity is in agreement with the simulation results and the experimental findings for these fuels. The calculations seem to be very sensitive to the particle size distribution (PSD) of the collected ashes, as the results presented reveal. However, more work is needed in this respect in, first, further developing the code and second, the validation of the code.

The sensitivity analysis of selected code parameters revealed the influence of the PSD on the results generated by the code and in specific, on the deposition ratios. In addition, increased deposition ratios were predicted by the ADP under oxyfuel conditions in comparison to the standard air combustion conditions, while all the other parameters were kept constant. This result is in agreement with the observed experimental results.

The ADP tool is still missing the ability to numerically model the condensation phenomena so at this moment the code represents a substantial simplification of the reality. The ADP is being further developed and equipped with additional functionalities and validated for different fuels and sets of conditions.

Expanding the ADP with additional sub models able to simulate other physical phenomena would help the predictor to be a supplementary tool supporting any future experiments and measurements campaigns. More simulations creating particle groups with varying physical (PSD)and chemical (composition) properties would help to bring the predictor closer to the reality of industrial boilers. Especially the interactions of different particles sizes and densities and the influence of this on the deposition phenomena would be necessary to be investigated.

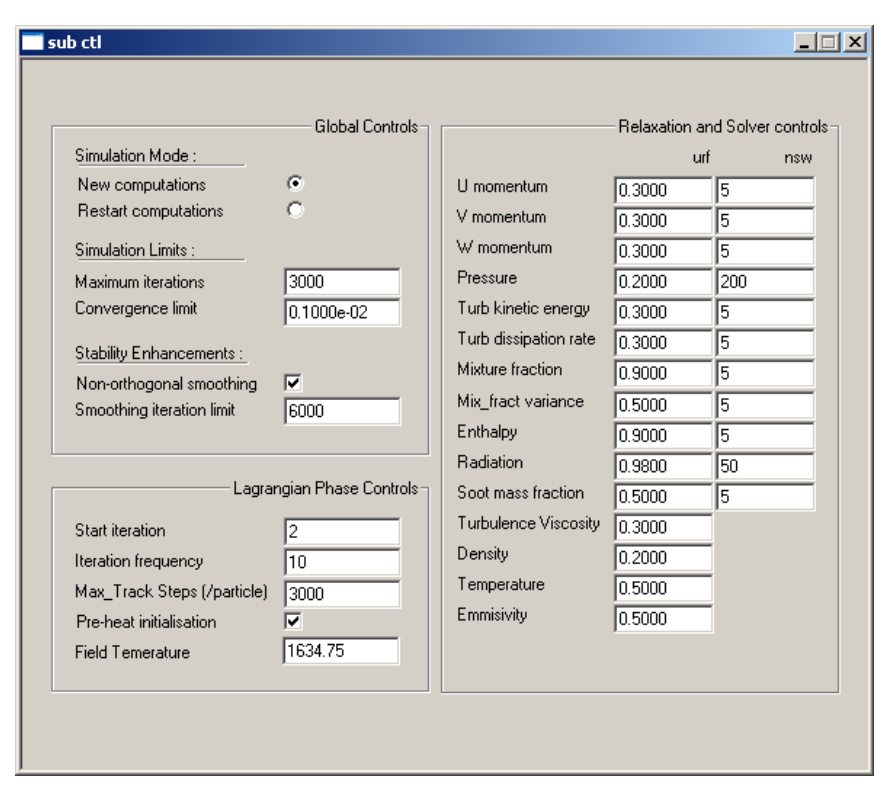
Experimental campaigns are proposed to obtain deposition data over a wide range of Stokes number (combinations of particle sizes, various gaseous environments) to validate the theoretical results of the ADP and the other relevant studies as well. Combinations of particle size, particle velocity and target cylinder size constitute a test matrix for these experiments which should cover a wide Stokes number range.

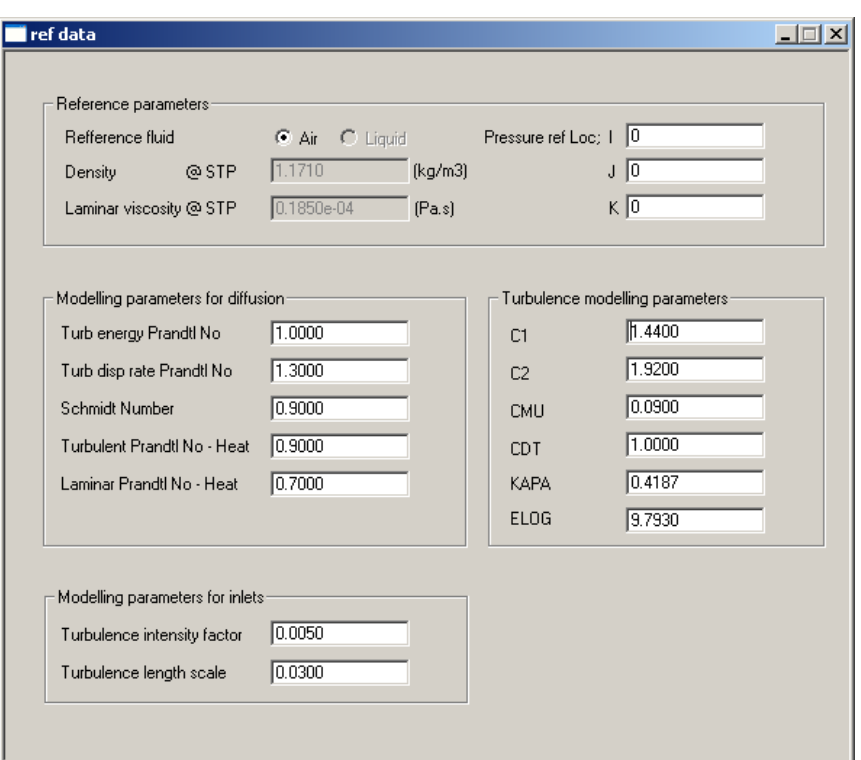
References

- Betrand C, Marco Losurdo, Rob Korbee, Mariusz Cieplik, Willem Van de Kamp "An Ash Deposition Post-processor for Biomass Co-Firing in Boilers or Furnaces", American Japanese Flame Research Committees International Symposium, Advances in Combustion Technologies: Improving the Environment and Energy Efficiency, Marriott Waikoloa, Hawaii October 22-24, 2007
- Doshi V., H.B. Vuthaluru, R. Korbee, J.H.A. Kiel "Development of a modeling approach to predict ash formation during co-firing of coal and biomass" Fuel Processing Technology 90 (2009) 1148-1156
- L. Fryda, C. Sobrino, M. Cieplik, W.L. van de Kamp, Study on ash deposition under oxyfuel combustion of coal/biomass blends , Fuel, Volume 89, Issue 8, August 2010, Pages 1889-1902
- Fryda L., C. Sorbino, M. Losurdo, M. Cieplik, W. de Jong., W.L. van de Kamp "Comparison of Ash Release and deposition under air vs. oxyfuel combustion of solid fuels" 1st Oxyfuel Combustion Conference
- Glazer M.P." Alkali metals in combustion of biomass with coal" PhD thesis, Delft University of Technology, 2007
- Hindiyarti L., F. Frandsen, H. Livbjerg, P. Glarborg, P. Marshall "An exploratory study of alkali sulfate aerosols formation during biomass combustion" Fuel 87 (2008) 1591-1600
- Jimenez S., J. Ballester "Formation of alkali sulphate in biomass combustion" Fuel 86 (2007) 486-493
- Joller M., T. Brunner, I. Obernberger, "Modeling of aerosol formation during biomass combustion for various furnace and boiler types", Fuel Processing Technology 88 (2007) 1136-1147
- Jordal K., Anheden M., Yan J. "Oxyfuel combustion of coal-fired power generation with CO2 capture opportunities and challenges" Greenhouse Gas Control Technology 2005; 7:201-9
- Korbee R., Losudro M., Cieplik M.K., Verhoeff F. "Monitoring and modelling of gas –side boiler fouling", 2007
- Lockwood F., Nasrullah M., Perrera S. "A computationally economical simulation of small particle deposition in a turbulent duct flow" in Combustion Technologies for a clean Environment Conference, Lisabon, Portugal 2002
- Lokare S.S., Dunaway J.D., Baxter L. "Investigation of ash deposition for a suite of biomass fuels and fuel blends" Energy & Fuels 2006, 20, 1008-1014

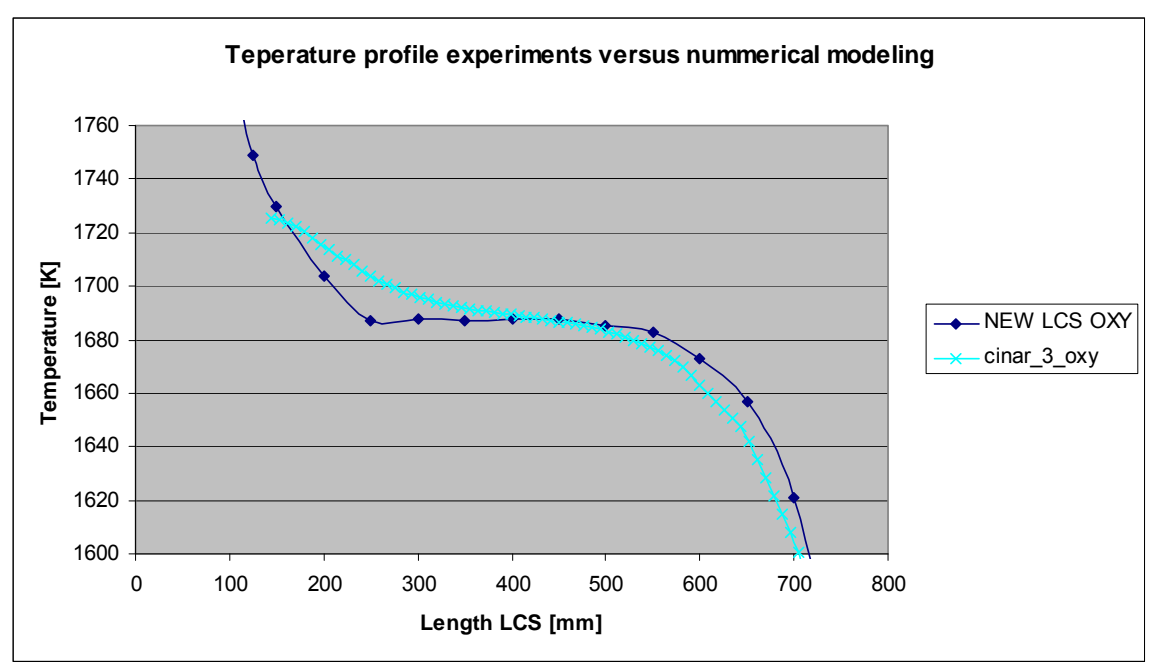
- Losurdo M. "Particle tracking and deposition from CFD simulations using a viscoelastic particle model" PhD Thesis, TUDelft, 2009
- Losurdo M., R. Korbee, B. Venneker, J. Kiel, and H. Spliethoff, "Ash and fouling deposition in pulverized co-firing biomass burners: CFD ash deposition modeling", *ECCOMAS*, Lisbon, 2005.
- Senior C.L., S. Srinivasachar "Viscosity of ash particles in combustion systems for prediction of particle sticking" Energy & Fuels 1995, 9, 277-283
- Srinivasachar S., L. Senior, J.J. Helbe and J.W. Monroe, in *Twenty-Fourth Symposium* (*International*) on *Combustion*, The Combustion Institute, Pittsburgh, 1179-1187 (1992).
- Shrinivas S. Lokare, A Mechanistic Investigation Of Ash Deposition In Pulverized-Coal And Biomass Combustion, PhD Thesis, Department of Chemical Engineering Brigham Young University, December 2008
- Wei Xiaolin, Christian Lopez, Thore von Puttkamer, Uwe Schnell, Sven Unterberger, and Klaus R. G. Hein "Assessment of Chlorine–Alkali–Mineral Interactions during Co-Combustion of Coal and Straw" Energy Fuels, 2002, 16 (5), pp 1095–1108
- Zheng Y., P.A. Jensen, A. D. Jensen, B. Sander, H. Junker "Ash transformation during co-firing coal and straw" Fuel 86 (2007) 1008-1020

Appendix A Other CINAR settings OXY-FUEL

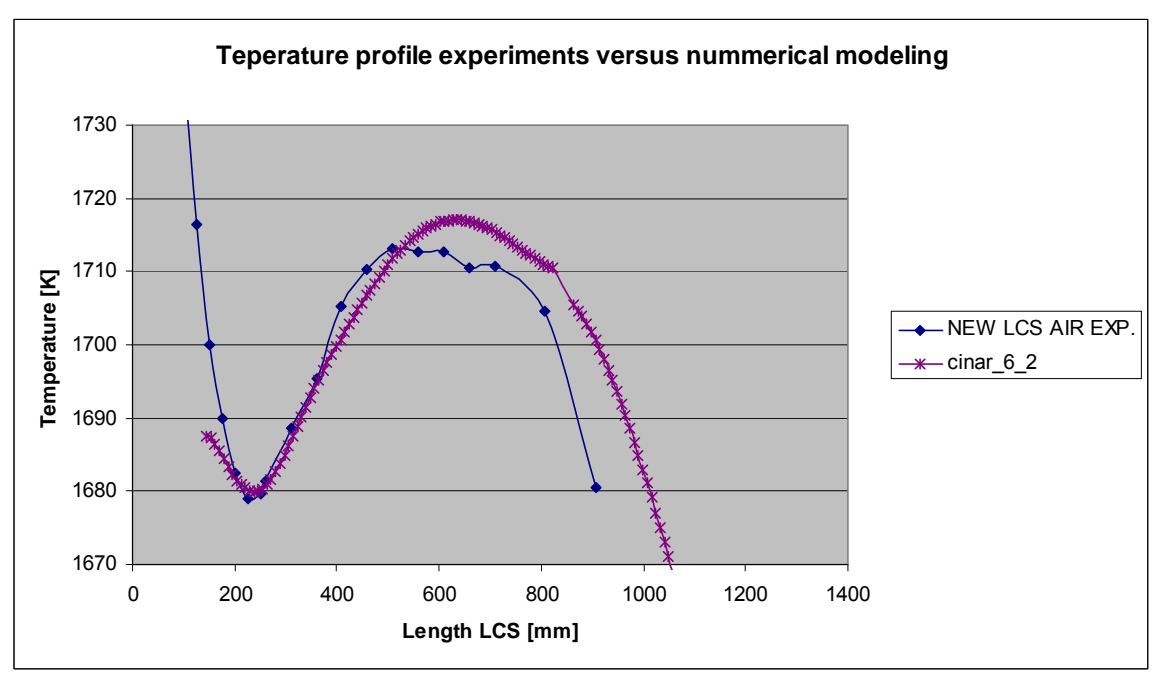




Appendix B Temperature profiles CINAR



Figuur B.1 Temperature profiles – atmospheric experiments (squares) and the fitting for the numerical simulation (stars)



Figuur B.2 Temperature profiles – atmospheric experiments (squares) and the fitting for the numerical simulation (stars)

Appendix C ADP – parameters

Particle Data File ==> PDF

TGN: 1

PNPG: 10000 (Particle Number Per Group)

@*************

Particle Size (Diameter): (S)

Mean: 27.76d-6 [m]

SD: 0.0d0 (Standard Deviation ==> Variance)

Particle Density: (D) Mean: 1900.d0 [kg/m3]

SD: 0.0d0 (Standard Deviation ==> Variance)

Particle Composition (Acid/Base Ratio): (C)

Mean: 0.711d0

SD: 0.0d0 (Standard Deviation ==> Variance)

Particle Specific Heat ==> PSH [J/(Kg*K)]

Mean: 840.d0 [J/(Kg*K)]

SD: 0.0d0 (Standard Deviation ==> Variance)

Particle Thermal Conductivity ==> PTC [W/(m*K)]

Mean: 0.14d0 [W/(m*K)]

SD: 0.0d0 (Standard Deviation ==> Variance)

Particle Young Modulus ==> PYM [Pa]

Mean: 70.d9 [Pa] (at 300 K)

SD: 0.0d0 (Standard Deviation ==> Variance)

Particle Temperature ==> PTemp [K]

Mean: 0.d0 [K] ==> Mean: 0.d0 ==> means particles get inlet cell's temperature

SD: 0.0d0 (Standard Deviation ==> Variance)

PCN: 1 (Particle Cluster Number)

PCC: S (Particle Cluster Criteria ===> Please select S,D or C)

Appendix D Other settings ADP

Particle Injection Location - PIL

```
ILN: 1 (Injection Location Number - integer number)
```

Inlet Box Coordinates

```
OBC_xmin= -4.0d-2
OBC_xmax= 4.0d-2
```

OBC_ymin= -4.0d-2 OBC_ymax= 4.0d-2

OBC_zmin= 1.0d0

OBC_zmax= 1.1d0

Appendix E Ash properties

LCS373	fa composition	.		6.1			f ii ii NDO	-
			, ,	w of elementl (g)	moles of element moles of oxide		r fraction oxide NBO/T	
CaO	40.078	56.078	3.34	13		0.324367483	0.035084673 -0.19	9323
MgO	20.305	36.305	3.7	6.6		0.325043093	0.035157749	
Na2O	22.99	61.98	2.27	3.1		0.067420618	0.00729244	
K20	39.098	94.196	2.35	13		0.166248913	0.017982039	
Al2O3	26.982	101.964	3.247	87		1.612185902	0.174379424	
SiO2	28.086	60.086	2.648	180		6.40888699	0.693206671	
TiO2	47.867	79.867	4.23	3.9		0.081475756	0.00881269	
Fe2O3	55.845	159.69	5.25	29		0.259647238	0.028084314	
				335.6		9.245275992	1	
LCS373	fa+s weighted average							
	w of element (g/mol)	w of oxide (g/mol)	density oxide (g/cm3)	w of elementl (g)	moles of element moles of oxide	e mola	r fraction oxide NBO/T	Ī
CaO	40.078	56.078	3.34	14.54682152		0.362962761	0.036485798 -0.18	3107
MgO	20.305	36.305	3.7	7.156855749	0.352467656	0.352467656	0.035430807	
Na2O	22.99	61.98	2.27	3.13093643		0.068093441	0.006844899	
K2O	39.098	94.196	2.35	13.61872861	0.348322897	0.174161448	0.017507084	
Al2O3	26.982	101.964	3.247	89.16555013	3.30463087	1.652315435	0.166094303	
SiO2	28.086	60.086	2.648	195.4682152	6.959631674	6.959631674	0.699597153	
TiO2	47.867	79.867	4.23	3.961872861	0.082768355	0.082768355	0.008320053	
Fe2O3	55.845	159.69	5.25	33.02173596	0.591310519	0.29565526	0.029719903	
						9.94805603	1	
LCS316	fa+s weighted average							
	w of element (g/mol)	w of oxide (g/mol)	density oxide (g/cm3)	w of elementl (g)	moles of element moles of oxide		r fraction oxide NBO/T	Ī
CaO	40.078	56.078	3.34	17.045	0.425295673	0.425295673	0.037151275 -0.17	7662
MgO	20.305	36.305	3.7	7.73	0.38069441	0.38069441	0.033255177	
Na2O	22.99	61.98	2.27	3.289	0.143062201	0.0715311	0.006248527	
K2O	39.098	94.196	2.35	14.77	0.377768684	0.188884342	0.016499801	
Al2O3	26.982	101.964	3.247	99.668	3.693869987	1.846934994	0.161337145	
SiO2	28.086	60.086	2.648	227.91	8.114719077	8.114719077	0.708853109	
TiO2	47.867	79.867	4.23	4.37	0.091294629	0.091294629	0.00797495	
Fe2O3	55.845	159.69	5.25	36.67	0.656638911	0.328319456	0.028680015	
						11.44767368	1	

LCS374							
	w of element (g/mol)	w of oxide (g/mol)	density oxide (g/cm3)	w of elementl (g)	moles of element moles of oxide	e mola	r fraction oxide NBO/T
CaO	40.078	56.078			0.432905834	0.432905834	0.042187301 -0.10582
MgO	20.305	36.305	3.7	9.12	0.449150456	0.449150456	0.043770363
Na2O	22.99	61.98	2.27	2.93	0.127446716	0.063723358	0.006209934
K2O	39.098	94.196	2.35	32.19	0.823315771	0.411657885	0.040116657
Al2O3	26.982	101.964	3.247	88.35	3.274405159	1.637202579	0.159547763
SiO2	28.086	60.086	2.648	193.49	6.889197465	6.889197465	0.671362273
TiO2	47.867	79.867	4.23	4.03	0.084191614	0.084191614	0.008204595
Fe2O3	55.845	159.69			0.586981825	0.293490912	0.028601115
						10.2615201	1
							•
LCS317							
				w of elementl (g)	moles of element moles of oxide		r fraction oxide NBO/T
CaO	40.078					0.4897949	0.04215481 -0.10715
MgO	20.305	36.305			0.511696626	0.511696626	0.044039809
Na2O	22.99	61.98	2.27	3.06	0.133101348	0.066550674	0.005727767
K2O	39.098	94.196	2.35	30.52	0.780602588	0.390301294	0.033591768
Al2O3	26.982	101.964	3.247	95.87	<mark>7</mark> 3.55310948	1.77655474	0.152901403
SiO2	28.086	60.086	2.648	223.51	7.958057395	7.958057395	0.684920151
TiO2	47.867	79.867	4.23	4.14	0.086489648	0.086489648	0.00744384
Fe2O3	55.845	159.69	5.25	37.92	0.679022294	0.339511147	0.029220451
						11.61895643	1
LCS446							
			, (3)	w of elementl (g)	moles of element moles of oxide		r fraction oxide NBO/T
CaO	40.078	56.078			<mark>'</mark> 0.989819851	0.989819851	0.075561579 -0.00580
MgO	20.305	36.305	3.7	21	1.034228023	1.034228023	0.078951642
Na2O	22.99	61.98	2.27	7.47	0.32492388	0.16246194	0.012402136
K2O	39.098	94.196	2.35	29	0.741725919	0.37086296	0.028311203
Al2O3	26.982	101.964	3.247	113.33	4.200207546	2.100103773	0.160319231
SiO2	28.086	60.086	2.648	219.98	7.832372	7.832372	0.597913241
TiO2	47.867	79.867	4.23	5.47	<mark>'</mark> 0.11427497	0.11427497	0.008723605
Fe2O3	55.845	159.69			0.990778046	0.495389023	0.037817363
						13.09951254	1

LCS374							
	w of element (g/mol)	w of oxide (g/mol)	density oxide (g/cm3)	w of elementl (g)	moles of element moles of oxide	e mola	r fraction oxide NBO/T
CaO	40.078	56.078			0.432905834	0.432905834	0.042187301 -0.10582
MgO	20.305	36.305	3.7	9.12	0.449150456	0.449150456	0.043770363
Na2O	22.99	61.98	2.27	2.93	0.127446716	0.063723358	0.006209934
K2O	39.098	94.196	2.35	32.19	0.823315771	0.411657885	0.040116657
Al2O3	26.982	101.964	3.247	88.35	3.274405159	1.637202579	0.159547763
SiO2	28.086	60.086	2.648	193.49	6.889197465	6.889197465	0.671362273
TiO2	47.867	79.867	4.23	4.03	0.084191614	0.084191614	0.008204595
Fe2O3	55.845	159.69			0.586981825	0.293490912	0.028601115
						10.2615201	1
							•
LCS317							
				w of elementl (g)	moles of element moles of oxide		r fraction oxide NBO/T
CaO	40.078					0.4897949	0.04215481 -0.10715
MgO	20.305	36.305			0.511696626	0.511696626	0.044039809
Na2O	22.99	61.98	2.27	3.06	0.133101348	0.066550674	0.005727767
K2O	39.098	94.196	2.35	30.52	0.780602588	0.390301294	0.033591768
Al2O3	26.982	101.964	3.247	95.87	<mark>7</mark> 3.55310948	1.77655474	0.152901403
SiO2	28.086	60.086	2.648	223.51	7.958057395	7.958057395	0.684920151
TiO2	47.867	79.867	4.23	4.14	0.086489648	0.086489648	0.00744384
Fe2O3	55.845	159.69	5.25	37.92	0.679022294	0.339511147	0.029220451
						11.61895643	1
LCS446							
			, (3)	w of elementl (g)	moles of element moles of oxide		r fraction oxide NBO/T
CaO	40.078	56.078			<mark>'</mark> 0.989819851	0.989819851	0.075561579 -0.00580
MgO	20.305	36.305	3.7	21	1.034228023	1.034228023	0.078951642
Na2O	22.99	61.98	2.27	7.47	0.32492388	0.16246194	0.012402136
K2O	39.098	94.196	2.35	29	0.741725919	0.37086296	0.028311203
Al2O3	26.982	101.964	3.247	113.33	4.200207546	2.100103773	0.160319231
SiO2	28.086	60.086	2.648	219.98	7.832372	7.832372	0.597913241
TiO2	47.867	79.867	4.23	5.47	<mark>'</mark> 0.11427497	0.11427497	0.008723605
Fe2O3	55.845	159.69			0.990778046	0.495389023	0.037817363
						13.09951254	1